

## Rotary motors sliding along surfaces

Alexander E. Filippov,<sup>1</sup> Andrea Vanossi,<sup>2</sup> and Michael Urbakh<sup>3</sup>

<sup>1</sup>*Donetsk Institute for Physics and Engineering of NASU, 83144, Donetsk, Ukraine*

<sup>2</sup>*CNR-INFM National Research Center S3 and Department of Physics, University of Modena and Reggio Emilia, Via Campi 213/A, 41100 Modena, Italy*

<sup>3</sup>*School of Chemistry, Tel Aviv University, 69978 Tel Aviv, Israel*

(Received 19 August 2008; revised manuscript received 9 December 2008; published 9 February 2009)

We introduce a family of molecular rotors that may convert light or chemical energy into directed translational motion along surfaces. The dependencies of diffusion coefficient and drift velocity of the rotating molecule on the magnitude of external torque, symmetry of surface potential, and temperature have been investigated. Our simulations show that the rotation-translation coupling could be very effective, and the molecule may move by approximately one surface lattice spacing per complete rotation. We have found that the unidirectionality of the rotary motion is not required to produce efficient directed sliding; this effect can be achieved by applying a time-periodic, or even randomly, oscillating torque which induces alternating molecular reorientations but does not generate complete rotations.

DOI: 10.1103/PhysRevE.79.021108

PACS number(s): 05.40.-a, 05.45.-a, 45.20.dc

In recent years there has been an increasing interest in studies of molecular rotary motors which function on surfaces [1–7]. Repetitive unidirectional rotary motion of macromolecules has been observed to occur under irradiation and chemical stimulations [3–6]. It has been demonstrated that the frequency of rotations can be controlled by photoexcitation processes, electric field, temperature, and molecular structure [3–6,8,9]. Tuning directionality of rotations presents so far the major difficulty. Molecular rotary motors functioning on surface are extremely interesting from a fundamental point of view [10–12] and could find applications in a variety of molecular-size devices and machines, for example, in the fields of nanofluidics, nanoelectronics, and nanophotonics [1,3–6,13].

In this work we demonstrate that molecule-surface interactions provide a strong coupling between rotational and translational degrees of freedom of macromolecules located on surfaces that may result in the rotation-induced enhancement of surface diffusion and directed translational motion. The latter requires asymmetry of the surface potential. The surface potential may be asymmetric, e.g., for substrates composed of dipole molecules or two kinds of different atoms or molecules.

It should be noted that the idea to excite an internal degree of freedom (in our case the rotational one) in order to induce a transport along another degree of freedom has been already discussed in the literature [7,11,14]. However, here we suggest a family of nanoscale motors that may convert molecular rotations or even reorientations into directed translational motion along the surfaces.

Our simulations show that for the optimal choice of system parameters the rotation-translation coupling could be very efficient, and the molecule may move by approximately one surface lattice spacing per a complete rotation. The effect of coupling between rotational and translational motions on surfaces has been recently discussed in the context of friction [15–17] unraveling new mechanisms of friction at both nanoscale and macroscale. We suggest to take advantage of this coupling in order to construct molecular rotors

that may convert light or chemical energy into directed motion along the surfaces.

In order to demonstrate the characteristic properties of translational motion induced by in-plane rotation of a macromolecule, we consider a molecule deposited on a surface which rotates under the action of an external torque. The dynamical behavior of the molecule is governed by the following coupled Langevin equations:

$$m\ddot{\mathbf{r}}_c + \nabla_{\mathbf{r}_c} U_m(\mathbf{r}_c, \phi) + \gamma\dot{\mathbf{r}}_c = \mathbf{f}_{r_c}(t), \quad (1)$$

$$I_z\ddot{\phi} + \nabla_{\phi} U_m(\mathbf{r}_c, \phi) + \Gamma\dot{\phi} - M_z = f_{\phi}(t). \quad (2)$$

The first equation describes the translational motion of the center of mass of the macromolecule of effective mass  $m$ , whose position is given by the two-dimensional coordinate  $\mathbf{r}_c = (x_c, y_c)$ ; Eq. (2) describes the rotation of the macromolecule having an effective moment of inertia  $I_z$  in the plane  $(x, y)$  with respect to the center of mass. The molecular rotation is induced by an external torque  $M_z$ , and the orientation of the macromolecule with respect to the underlying surface is given by a rotational angle  $\phi$ . The parameters  $\gamma$  and  $\Gamma$  are responsible for the dissipation of the macromolecule's kinetic energy due to the translational and rotational motion, respectively. The effect of thermal fluctuations on the translational and rotational motion of the molecule is given by the random force and torque,  $\mathbf{f}_{r_c}(t)$  and  $f_{\phi}(t)$ , which are  $\delta$ -correlated,  $\langle f_{r_c,i}(t)f_{r_c,j}(t') \rangle = 2\gamma k_B T \delta(t-t') \delta_{i,j}$  and  $\langle f_{\phi}(t)f_{\phi}(t') \rangle = 2\Gamma k_B T \delta(t-t')$ , where  $i, j = x, y$ .

The macromolecule is treated as a rigid body, which contacts with the substrate through the two-dimensional (2D) layer including  $N$  atoms. The layer is modeled as a finite lattice, composed of hexagonal rings [see Fig. 1(a)]. The interaction between a single atom in the molecule and the underlying surface is simulated by the effective potential,

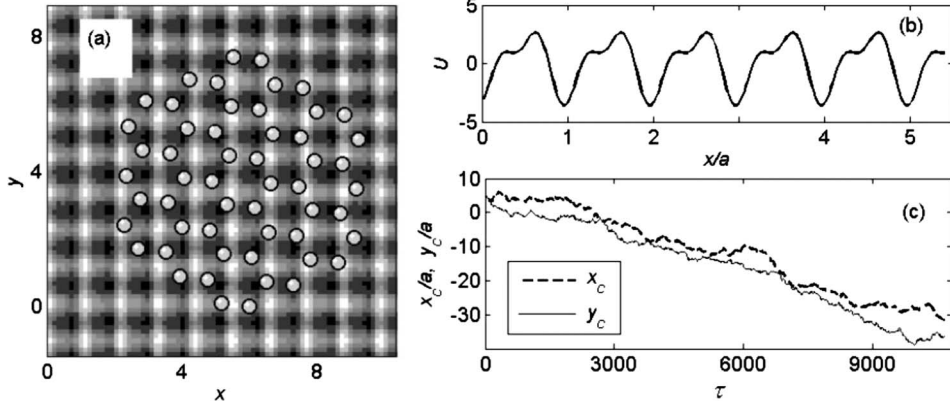


FIG. 1. The 54-atom symmetric macromolecule on the surface. (a) Schematic view of the system. The substrate potential is shown by the gray-scale map. (b) Cross section of the surface potential along the  $x$  direction for the misfit angle  $\theta=\pi/4$ . (c) Solid and dashed curves show time dependences of the displacement of the center of mass in  $x$  and  $y$  directions, respectively. Parameter values:  $A_x=A_y=1$ ,  $N=54$ ,  $\theta=\pi/4$ ,  $a_1/a=0.74$ ,  $M_z/(I_z\omega_0^2)=0.104$ ,  $\gamma/(m\omega_0)=0.78$ ,  $NU_0/(I_z\omega_0^2)=0.04$ ,  $k_B T/U_0=0.04$ .

$$U(x,y) = -U_0[\cos(2\pi x/a) + A_x \cos(4\pi x/a + \theta)/2 + \cos(2\pi y/a) + A_y \cos(4\pi y/a + \theta)/2], \quad (3)$$

where  $U_0$ ,  $U_0 A_x/2$ , and  $U_0 A_y/2$  are the amplitudes of the harmonics constituting the surface potential,  $a$  is a period of the substrate square lattice, and  $\theta$  is the misfit angle which controls the asymmetry of the potential. For  $\theta \neq n\pi/2$  ( $n=0, \pm 1, \pm 2, \dots$ ) and  $A_x, A_y \neq 0$  we have an asymmetric, ratchet-type potential. The gray scale map of  $U(x,y)$  is shown in Fig. 1(a), where dark and light gray colors correspond to minima and maxima of the potential, respectively. Cross section of the surface potential along the  $x$  direction for  $\theta=\pi/4$  and  $A_x=A_y=1$  is shown in Fig. 1(b).

In a rigid molecule, the relative positions of the atoms are fixed with respect to the coordinate of its center of mass and, as a result, the molecule-surface interaction is described by an effective potential  $U_m(x_c, y_c, \phi)$ , with the corresponding force  $\nabla_{r_c} U_m$  and torque  $\nabla_{\phi} U_m$  which are simply obtained by summing  $U(x,y)$  and the moments over  $N$  atomic contributions in the macromolecule.

As an example, we present below the results obtained for a 54-atom symmetric molecule [see Fig. 1(a)]. However, our simulations have demonstrated that the main conclusions of this work are robust and hold for a broad range of systems: symmetric and asymmetric rigid molecules of different sizes, flexible molecules, and even nano-objects with disordered structures. For all these systems we have found that when the magnitude of the external torque  $M_z$  exceeds some threshold value, the molecule performs a rotational motion which gives rise to an enhanced diffusion on symmetric surfaces and to a directed translational motion on asymmetric ones [see Fig. 1(c)]. These effects have been found for both a permanent external torque,  $M_z \equiv \text{const}$ , which causes a unidirectional rotation of the molecule, as well as for a periodic, or even randomly, oscillating torque which induces alternating molecular reorientations but does not generate a complete rotation. In what follows, we use the dimensionless coordinates, time and torque:  $\tilde{x}_c = x_c/a$ ,  $\tilde{y}_c = y_c/a$ ,  $\tau = t\omega_0$ , and  $\tilde{M}_z = M_z/(I_z\omega_0^2)$ , where  $\omega_0 = \Gamma/I_z$ .

Figure 1(c) shows a typical trajectory of the center of mass of the molecule which has been calculated for the case of the permanent external torque. The solid and dashed curves present displacements in the  $x$  and  $y$  directions, respectively. The figure clearly demonstrates that the molecule rotations induce a directed translational motion whose direction depends on the ratio of amplitudes  $A_x$  and  $A_y$  in the potential (3) and on the misfit angle  $\theta$ . Below we focus on the consideration of the case  $A_x=A_y$ , when the time-averaged velocities in  $x$ - and  $y$  directions should be equal in the limit  $t \rightarrow \infty$ .

It should be noted that even under the influence of the permanent torque the frequency of the molecular rotation,  $\Omega = \dot{\phi}$ , changes in time, and the molecule performs a correlated rotational-translational motion. The dynamics of the molecular translational motion can be represented as a set of alternating stick and slip segments. During the stick intervals the center of mass is trapped in minima of the potential  $U_m(r_c, \phi)$  but the molecule continues to rotate, and with time it approaches a more favorable mismatched configuration with a reduced barrier for the translational motion. Then the molecule can overcome the barrier with help of thermal fluctuations and slip to an adjacent trapped state. The asymmetry of the molecule-surface potential,  $U_m(r_c, \phi)$ , gives rise to a statistically preferable direction of slips. The described dynamics has a diffusive nature for centrosymmetric potentials ( $\theta \neq n\pi/2$  or  $A_x, A_y=0$ ), and exhibits a directional translation motion for asymmetric surfaces.

Figure 2 shows the dependencies of diffusion coefficient,  $D$ , time-averaged drift velocity,  $\langle v_{\parallel} \rangle$ , and angular frequency,  $\langle \Omega \rangle$ , on the magnitude of the external torque,  $M_z$ . The diffusion coefficient,  $D = \lim_{t \rightarrow \infty} \frac{1}{4t} \langle |\mathbf{r}_c(t) - \mathbf{r}_c(0)|^2 \rangle$ , has been calculated for the centrosymmetric surface,  $\theta=0$ , while  $\langle v_{\parallel} \rangle$  and  $\langle \Omega \rangle$  have been calculated for the asymmetric surface with  $\theta=\pi/4$ . One can see that in order to initiate the molecular rotation the torque should exceed some threshold value,  $M_z^{\text{stat}}$  [ $\approx 0.1 I_z \omega_0^2$  in Fig. 2(c)], which is required to overcome the potential barriers restricting the rotations of the molecule with respect to the surface. An origin of the threshold torque is analogous to that for the static friction in the case of trans-

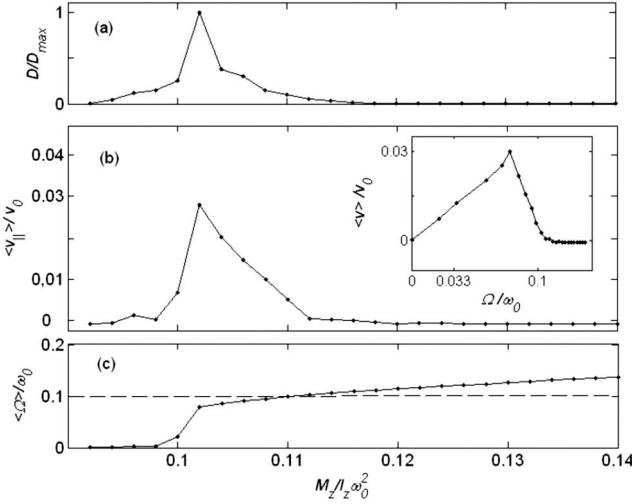


FIG. 2. Dependencies of the dimensionless diffusion coefficient (a), time-averaged drift velocity (b), and angular frequency (c) on the dimensionless torque,  $M_z/(I_z\omega_0^2)$ .  $D$  has been calculated for the centrosymmetric surface,  $\theta=0$ , while  $\langle v_{\parallel} \rangle$  and  $\langle \Omega \rangle$  have been calculated for the asymmetric surface with  $\theta=\pi/4$ . The diffusion coefficient is normalized to its maximal value  $D_0$ , and the drift velocity to  $v_0=\omega_0 a$ . Inset to (b) shows  $\langle v_{\parallel} \rangle$  vs  $\Omega$  for the molecule rotating with a constant angular frequency. Parameter values as in Fig. 1.

lation motion, and, as the static friction,  $M_z^{\text{stat}}$  depends on the system parameters such as molecular-surface interaction, commensurability, temperature, etc. When the external torque exceeds the threshold value the mean angular frequency increases as a function of  $M_z$  and with it the diffusion coefficient and the mean drift velocity. However, whereas  $\langle \Omega \rangle$  grows monotonically with  $M_z$ , both  $D$  and  $\langle v_{\parallel} \rangle$  exhibit maxima as a function of  $M_z$ . This effect results from the fact that for high enough  $\langle \Omega \rangle$  the lifetime of the configurations with the low translational barriers becomes shorter than the characteristic slip time, and the transformation of the rotational motion to the translational one turns out to be ineffective [see inset in Fig. 2(b)].

Above  $M_z^{\text{stat}}$ , the model exhibits two regimes of rotational motion as a function of  $M_z$ : (i) for  $0.1 < M_z/I_z\omega_0^2 < 0.11$  time intervals of rotation alternate with motionless ones, and the fraction of rotational intervals increases with  $M_z$ ; (ii) for  $M_z/I_z\omega_0^2 > 0.11$  the molecule rarely, if ever, stops to rotate and  $\langle \Omega \rangle \approx M_z/\Gamma$  [see Fig. 2(c)]. For the high values of the torque,  $M_z/I_z\omega_0^2 > 0.11$ , the molecule rotates fast and does not respond to the potential corrugation, as a result both the diffusion coefficient and drift velocity are negligible.

Figure 2(a) demonstrates that the diffusivity may be strongly enhanced by the molecular rotations. For the chosen values of the parameters the bare diffusivity ( $D$  in the absence of rotations) is negligible and has not been detected at the time scale of our simulations. The maximal value of the rotation-induced diffusion coefficient is even few times higher than the free diffusivity of the molecule,  $D_{\text{free}}=k_B T/(N\gamma)$ . The maximal drift velocity in Fig. 2(b) corresponds to a remarkable one lattice constant displacement of the molecule per three complete rotations.

The results presented in Fig. 2 have been obtained for a

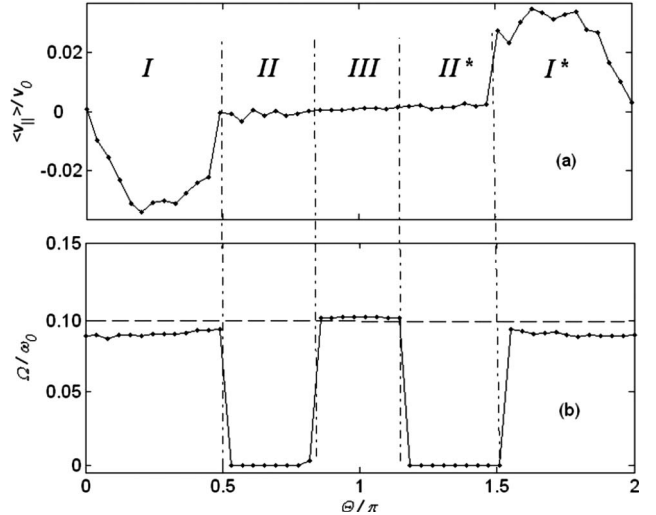


FIG. 3. Dependencies of the mean drift velocity (a), and angular frequency (b) on the misfit angle,  $\theta$ . Parameter values as in Fig. 1.

finite temperature,  $k_B T=0.04U_0$ . However, the enhancement of the diffusivity and directed translational motion has been also found for an infinitesimal low temperature. This is explained by the fact that rotations bring the molecule to the configurations where the barrier for the translation motion diminishes and then even a weak noise may generate a slip of the molecule to the neighboring minima of the potential. The increase of temperature leads to a reduction of the threshold value of the torque,  $M_z^{\text{stat}}$ , and for moderate temperatures,  $k_B T \leq 0.5U_0$ , the angular frequency grows with  $T$ . Also the probability of translational slips (jumps) over the potential barriers increases with  $T$ . As a result, for the moderate temperatures the diffusion coefficient and the drift velocity grow with  $T$ . For higher temperatures the molecular motion gets erratic, and  $\langle v_{\parallel} \rangle$  decreases. Finally for  $k_B T \geq U_0$  the motion loses completely the directionality and becomes diffusive.

The efficiency of the rotation-translation motor strongly depends on the misfit angle  $\theta$  which controls the asymmetry of the surface potential. Figure 3 shows dependences of the mean angular frequency and drift velocity on  $\theta$  for a given value of the torque,  $M_z=0.104I_z\omega_0^2$ , which corresponds to the maximum of  $\langle v_{\parallel} \rangle$  for  $\theta=\pi/4$ . One can see that the velocity is antispecular with respect to  $\theta=\pi$ , namely  $\langle v_{\parallel}(\pi-\theta) \rangle = -\langle v_{\parallel}(\pi+\theta) \rangle$ , and there are well-defined windows of  $\theta$  where  $\langle v_{\parallel} \rangle$  is not zero [I and I\* in Fig. 3(a)]. The drift velocity vanishes in the intervals, II, II\*, and III for two different reasons. In the intervals II and II\* after some transient time the molecule becomes locked in configurations with high barriers for the rotational motion, and it ceases to rotate and move translationally. In the interval III the mean angular frequency exceeds the critical value above which the rotations become too fast and do not allow enough time for the translational slips from one potential valley to another. This critical frequency is marked by a horizontal dashed line in Fig. 3(b), and its value agrees well with the upper limiting frequency for the rotation-translation coupling which has been found in calculations of  $\langle v_{\parallel} \rangle$  as a function of  $M_z$  [see inset in Fig. 2(b)].

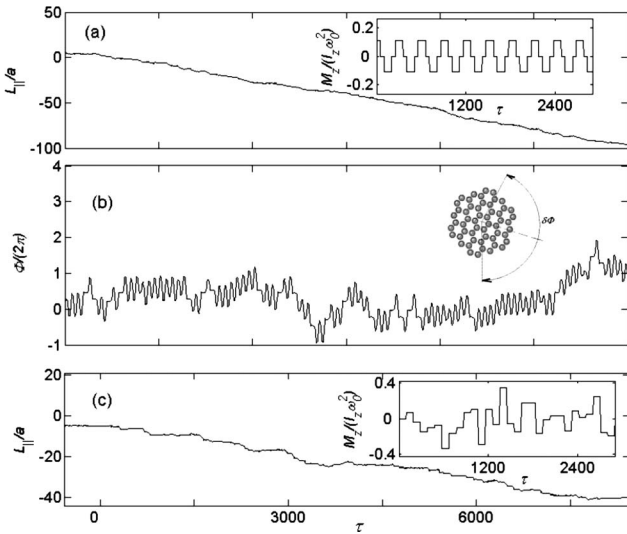


FIG. 4. Directed translational motion under the action of the periodically and randomly oscillating torque. (a) and (c) show the displacement,  $L_{\parallel}/a$ , of the center of mass for the periodic and random variation of the torque, respectively; (b) the variation of the rotational angle for the periodic torque. Insets to (a) and (c) show time variations of the periodic and randomly changed torque. Parameters as in Fig. 1.

Our calculations show that the direction of the translational motion remains the same for both clockwise and anti-clockwise external torques. This observation has important implications for experimental realizations of the rotation-translation motor proposed here. As we have already noted above the major difficulty in operating molecular rotors lies not in achieving molecular rotations but in controlling their directionality, namely producing repetitive unidirectional ro-

tations. We have found that the unidirectionality of the rotary motion is not required to produce efficient directional translations. Figure 4 demonstrates that the same effect can be achieved applying an oscillatory torque which induces alternating molecular reorientations but does not generate complete rotations. In order to induce the translational motion the reorientation angle should be large enough to allow for a slip of the molecule center of mass between two adjacent potential valleys during a half-period of the torque oscillations. Then during the next half-period the torque has the opposite direction but the slip preferably occurs in the same direction as before.

The main conclusions of this work hold also for a randomly rotated macromolecule. As a possible scenario, we assumed the torque to vary randomly by following the trace of a random walker with the same characteristic time steps and jump amplitudes as in the previous example of the periodic torque [see inset to Fig. 4(c)]. Figure 4(c) shows that in this case the mean drift velocity is somewhat lower than for the periodic torque, but still the transport turns anyway to be very efficient. Besides, the depicted scenario turns to be even more robust since symmetry, disordered structure, or rigidity of macromolecules seem not to be crucial ingredients for the observed dynamical features.

This work, as part of the European Science Foundation EUROCORES Programme FANAS, was supported from funds by the Israel Science Foundation and the EC Sixth Framework Programme, under Contract No. ERAS-CT-2003-980409. A.V. gratefully acknowledges the financial support of the European Commissions NEST Pathfinder program TRIGS under Contract No. NEST-2005-PATH-COM-043386 and thanks the School of Chemistry at Tel Aviv University for the kind hospitality.

---

[1] J. K. Gimzewski, C. Joachim, R. R. Schlittler, V. Langlais, H. Tang, and I. Johannsen, *Science* **281**, 531 (1998).  
 [2] C. Joachim and J. K. Gimzewski, *Struct. Bonding (Berlin)* **99**, 1 (2001).  
 [3] R. A. van Delden, M. K. J. ter Wiel, M. M. Pollard, J. Vicario, N. Koumura, and B. L. Feringa, *Nature (London)* **437**, 1337 (2005).  
 [4] W. R. Browne and B. L. Feringa, *Nat. Nanotechnol.* **1**, 25 (2006).  
 [5] D. A. Leigh, F. Zerbetto, and E. R. Kay, *Angew. Chem., Int. Ed.* **46**, 72 (2007).  
 [6] V. Balzani, A. Credi, and M. Venturi, *ChemPhysChem* **9**, 202 (2008).  
 [7] M. Porto, M. Urbakh, and J. Klafter, *Phys. Rev. Lett.* **84**, 6058 (2000).  
 [8] M. F. Hawthorne *et al.*, *Science* **303**, 1849 (2004).  
 [9] G. S. Kottas, L. I. Clarke, D. Horinek, and J. Michl, *Chem. Rev. (Washington, D.C.)* **105**, 1281 (2005).  
 [10] F. Julicher, A. Ajdari, and J. Prost, *Rev. Mod. Phys.* **69**, 1269 (1997).  
 [11] P. Reimann, *Phys. Rep.* **361**, 57 (2002).  
 [12] R. D. Astumian and P. Hanggi, *Phys. Today* **55**, 33 (2002).  
 [13] D. Fleishman, J. Klafter, M. Porto, and M. Urbakh, *Nano Lett.* **7**, 837 (2007).  
 [14] See, e.g., M. Bier, M. Kostur, I. Derenyi, and R. D. Astumian, *Phys. Rev. E* **61**, 7184 (2000), and references therein.  
 [15] A. E. Filippov, M. Dienwiebel, J. W. M. Frenken, J. Klafter, and M. Urbakh, *Phys. Rev. Lett.* **100**, 046102 (2008).  
 [16] Z. Farkas, G. Bartels, T. Unger, and D. E. Wolf, *Phys. Rev. Lett.* **90**, 248302 (2003).  
 [17] P. D. Weidman and C. P. Malhotra, *Phys. Rev. Lett.* **95**, 264303 (2005).